



# Gain enhancement of a novel $1 \times 2$ microstrip patch antenna array based on cylindrical and cuboid photonic crystal substrate in THz

Mohamed Elamine Benlakehal<sup>1</sup> · Abdesselam Hocini<sup>2</sup> · Djamel Khedrouche<sup>2</sup> · Mohamed Nasr eddine Temmar<sup>2</sup> · Tayeb Ahmed Denidni<sup>3</sup>

Received: 27 January 2022 / Revised: 18 August 2022 / Accepted: 3 January 2023 / Published online: 11 January 2023  
© The Author(s), under exclusive licence to Springer Science+Business Media, LLC, part of Springer Nature 2023

## Abstract

Recent advancements in the next-generation wireless communication technologies require high gain and larger bandwidth. In this paper, a high gain novel  $1 \times 2$  circular microstrip patch antenna array is proposed to operate around 0.65 THz based on different substrates. First, the proposed antenna array is designed based on air cylinders holes embedded in a thick polyimide substrate, and then by using air cuboids holes. The proposed antenna array model is compared with a homogeneous polyimide substrate. The simulation results showed that the performance of the proposed antenna array was enhanced especially by using air cuboids holes and achieved a minimal return loss of  $-74.10$  dB, a wide bandwidth greater than 290 GHz, a gain of 10.57 dB, and radiation efficiency of 82.96% at a resonance frequency of 0.65 THz. Next, the gain of the proposed antenna array is investigated further by using two different substrates with a modified non-periodic photonic crystal where the air cylinders holes and air cuboids holes are mixed at the same time and embedded in the substrate with different diameter values. The simulation showed an enhancement in the gain where the highest gain was achieved by antenna array 4 of 12.03 dB. The proposed antenna array can be useful in imaging, sensing, and next-generation wireless communication technologies. The simulation is carried out by using the CST Microwave Studio simulator.

**Keywords** Microstrip patch antenna array · CST · Photonic crystal · THz band · Terahertz application · Radiation characteristic

✉ Mohamed Elamine Benlakehal  
m.benlakehal@univ-boumerdes.dz  
Abdesselam Hocini  
abdesselam.hocini@univ-msila.dz  
Djamel Khedrouche  
djamel.khedrouche@univ-msila.dz  
Mohamed Nasr eddine Temmar  
temmar.mohamed@univ-msila.dz  
Tayeb Ahmed Denidni  
denidni@emt.inrs.ca

<sup>1</sup> Laboratoire d'ingénierie des Systèmes et Télécommunication, Department of Electrical Engineering Systems, University of M'hamed Bougara Boumerdes, 35000 Boumerdes, Algeria

<sup>2</sup> Laboratoire d'Analyse des Signaux et Systèmes, Département d'Electronique, Université Mohamed Boudiaf - M'Sila, Route Ichebilia, BP. 166, 28000 M'sila, Algeria

<sup>3</sup> Energie, Matériaux, Télécommunications, Institut National de la Recherche Scientifique (INRS), Montreal, Canada

## 1 Introduction

Over the last decade, the THz frequency band (0.1 THz–10 THz) has gained a remarkable research interest because of its unique properties compared to micro-millimeter waves, such as high spectral resolution, non-ionizing, larger bandwidth, high-speed data transmission up to 100 Gbps, and low power consumption [1–5]. This frequency band has a significant contribution to many necessary applications including the next-generation communication networks [6], defense and security screening [7, 8], imaging [9], medical diagnostic [10], and atmospheric spectroscopy [11]. Unfortunately, the THz frequency band suffers from a high path loss and signal attenuation caused by the atmosphere due to water vapor absorption at high frequencies [12]. Therefore, to use the THz frequency band efficiently, high gain transmitting and receiving devices are primary aspects. There are nine low-attenuation windows in the frequency range of 0.1–3 THz of the spectrum where the path loss is comparatively small, THz transmission could be established

at these low-attenuation windows to enhance the wireless link reliability. One of these windows exists around 0.65 THz which has taken interest by many researchers in recent years [13]. The antenna is one of the most critical components of THz research and technology advancement that can achieve unidirectional radiation with high gain [14]. Different antenna structures have been discussed in the THz frequency band, including, Yagi antenna [15], bow-tie antenna [16], lens integrated antenna [17], metallic horn antenna [18], on-chip antenna [19], dipole antenna [20], and Leaky wave antenna [21]. However, there are still complications in structure design and size miniaturization. Microstrip patch antennas offer greater potential for integration as compared to the other antenna structures candidates for THz applications [22–24] because of their low profile, low cost, high compatibility with integrated circuit technology, ease to design and fabrication [25–27]. Unfortunately, the conventional patch antenna suffers from strong surface waves which deteriorate the patch antenna performance resulting in low gain and narrow bandwidth [28]. In order to enhance the gain and realize better radiation characteristics of the patch antenna, a variety of approaches have been investigated over the years by many researchers. Commonly used approaches are antenna array configuration [29], multilayered substrate technique [30], defected ground [31], metamaterial technique [32], epsilon-near-zero (ENZ) metamaterials [33], and photonic crystals structures [34–37]. Therefore, a patch array design with photonic crystals is definitely helpful in improving the performance of the patch antenna. The photonic crystal structures are also known as photonic band gap (PBG) structures, which are artificial materials made of periodic implants within a surrounding medium of a hollow air cylinder having circular, square, hexagonal, triangular, and elliptical in shape which are implanted in the dielectric substrate material. These structures have been developed in which electromagnetic wave propagation in any direction is completely prevented for all frequencies within a stop band [38]. There are different structures types of PBG such as 1D, 2D, or 3D. Two-dimensional (2D) photonic crystals have gained the most interest from many researchers, as they are much easier to fabricate and design compared to three-dimensional (3D) photonic crystals and have promising applications in planar waveguides, optical and microwave cloak [39, 40].

Previously, Kushwaha et al. [28] designed a novel microstrip patch antenna based on photonic crystals and polyimide substrate and obtained a gain of 7.934 dB, a resonance frequency of 0.6308 THz, and bandwidth of 36.25 GHz. Also, Hocini et al. [33] designed a rectangular microstrip patch antenna based on periodic and aperiodic photonic crystals with polyimide substrate around 0.65 THz which yielded the gains of 8.95 dB and 9.19 dB, respectively, and bandwidth greater than 230 GHz. Unfortunately, the low gain is

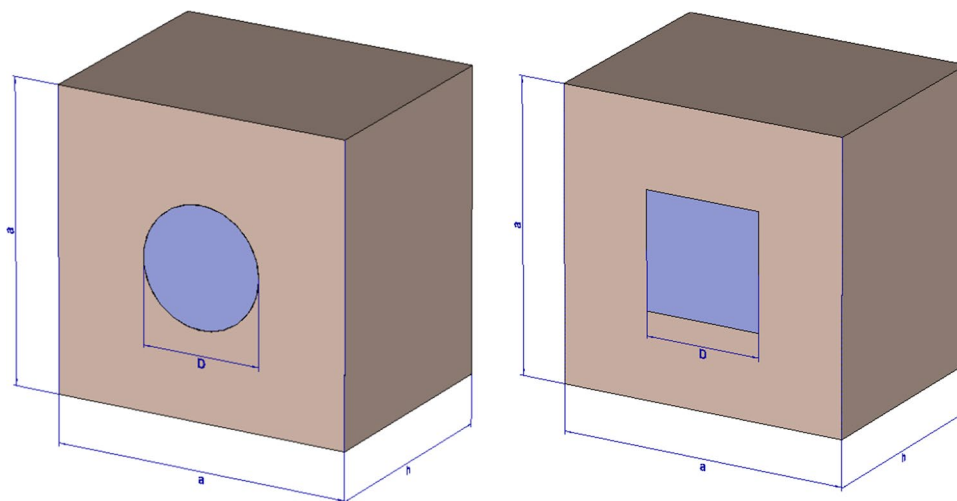
still the main problem that can not meet the requirement of the next-generation wireless communication technologies. In this paper, a novel  $1 \times 2$  circular microstrip patch antenna array with a corporate feeding technique instead of a single rectangular patch is proposed to achieve high gain and better radiation characteristics around 0.65 THz. The proposed antenna array is designed based on the photonic crystals that include air cylinders holes, air cuboids holes, and mixed air cylinders holes with air cuboids holes embedded in a thick polyimide substrate, which can be useful in imaging, sensing, and next-generation wireless communication technologies. This paper is organized as the following: In Sect. 2, we investigated and compared the radiation characteristics of the  $1 \times 2$  circular microstrip patch antenna array to the conventional one by defining two different photonic crystals substrate including air cylinders holes and air cuboids holes. In Sect. 3, we describe two different enhancements to the photonic crystal substrate by mixing the air cylinders holes with the air cuboids holes with different diameter values to improve the gain of the proposed antenna array. Finally, we concluded our work in Sect. 4.

## 2 Antenna array design based on cylindrical and cuboid photonic crystal substrate

Microstrip patch antenna comes in various shapes like rectangular, circular, triangular, and other irregular shapes too that can be fed by various feeding techniques [41]. In this study, a  $1 \times 2$  microstrip patch antenna array is proposed which consists of two identical radiating patches which are circular in the shape of radius 195  $\mu\text{m}$  designed with the parallel feed arrangement and separated by a distance of 690  $\mu\text{m}$ . The parallel or corporate feed has a single input port and multiple feed lines in parallel with the output port, each of these feed lines is terminated at an individual radiating patch [42]. Impedance matching techniques can be categorized into two broad categories i.e. Distributed Method and Lumped Element Method. Distributed Method can be done by structural modification via stubs and transformer, however, this method increases the size of the antenna and is not recommended for array systems. Lumped Element Method can be done by inserting a matching network i.e. inductor and capacitor, which is introduced to realize impedance matching between antenna array patches and feed structures [43]. The resonant input resistance of the edgefed patch antenna array can be easily tuned to 50  $\Omega$ . Therefore, the width of the feed network  $W$  is given by [44]:

$$W = \exp\left(\frac{Z_c}{87\sqrt{\epsilon_r + 1.41}}\right) \frac{0.8}{5.98h} \quad (1)$$

**Fig. 1** The geometry of the unit cell



(a) The geometry of an air cylinder hole.

(b) The geometry of an air cuboid hole.

where  $Z_c$  is the impedance of the feed line  $W$ ,  $\epsilon_r$ , and  $h$  are the dielectric constant and the height of the substrate material, respectively. The lengths  $L$  and  $L_f$  provide impedance transformation and phase matching on the radiated patches, respectively, which can be obtained using the following formulas [44]:

$$L = (2P + 1) \times \frac{\lambda}{4} \tag{2}$$

$$L_f = (2Q + 1) \times \frac{\lambda}{2} + 2\Delta L \tag{3}$$

where  $P$  and  $Q$  are non-negative integers (in our work we chose  $P = Q = 1$ ),  $\lambda$  is the operating wavelengths and  $\Delta L$  is patch length extension due to the fringing field effect [45]. The proposed antenna array structure is designed based on the photonic crystal substrate whose host material is polyimide where  $\epsilon_r=3.5$  and  $\tan \delta = 0.0027$  of thickness  $85 \mu\text{m}$ . The photonic crystal structure is made of air cylinders holes and air cuboids holes embedded in a polyimide dielectric material. The geometric configuration of the air cylinder hole and air cuboid hole embedded in the dielectric substrate unit cell is shown in Fig. 1. The dimensions of the square unit cell for both the air cylinder hole and air cuboid hole are similar of  $109 \times 109 \mu\text{m}^2$  with a lattice constant and diameter of  $109 \mu\text{m}$  and  $44 \mu\text{m}$ , respectively, and thickness of  $85 \mu\text{m}$ . Hence, the proposed 1x2 microstrip patch antenna array structure is designed based on two different photonic crystal substrates, antenna array 1 is designed based on periodic air cylinders holes and antenna array 2 is designed based on periodic air cuboids holes. Antenna array 0, namely a conventional antenna array based on the homogeneous polyimide substrate, which is designed and simulated for comparison and analysis purposes. Figure 2 shows the structures of antenna array 0, antenna array 1, and antenna array 2 based on the

**Table 1** Parameter values for antenna array 0 based on a homogeneous substrate, antenna array 1, and antenna array 2 based on a periodic PBG substrate

Parameter	Value ( $\mu\text{m}$ )	
	Antenna array 0	Antenna arrays 1 and 2
Patch radius ( $R$ )	180	195
Distance between patches ( $d$ )	565	690
Substrate thickness ( $h$ )	85	85
Lattice constant ( $a$ )	**	109
Substrate width ( $W_s$ )	$14 \times a$	$14 \times a$
Substrate length ( $L_s$ )	$9 \times a$	$9 \times a$
Cylinder/Cuboids diameter ( $D$ )	**	44
Width of $50 \Omega$ microstrip line ( $W$ )	235	235
Length of $50 \Omega$ microstrip line ( $L$ )	160	160
Width of $100 \Omega$ line to the patch ( $W_p$ )	15	15
Length of $100 \Omega$ line to the patch ( $L_p$ )	150	111.4

homogeneous and periodic PBG substrates, respectively. The physical dimension of each element is shown in Table 1. The thickness of the employed metal was  $0.5 \mu\text{m}$ . The radiation characteristics of the proposed antenna arrays 0, 1, and 2 are investigated and analyzed around  $0.65 \text{ THz}$  using the CST Microwave Studio in terms of return loss, bandwidth, gain, directivity, and radiation efficiency. Figure 3 shows the return loss versus the frequency for the different antenna array configurations, which indicates that antenna array 0 had a return loss of  $-20.75 \text{ dB}$  at a resonance frequency of  $0.63 \text{ THz}$  and bandwidth greater than  $194 \text{ GHz}$ , whereas, antenna array 1 achieved a return loss of  $-33.85 \text{ dB}$  at a resonance frequency of  $0.637 \text{ THz}$  and bandwidth greater

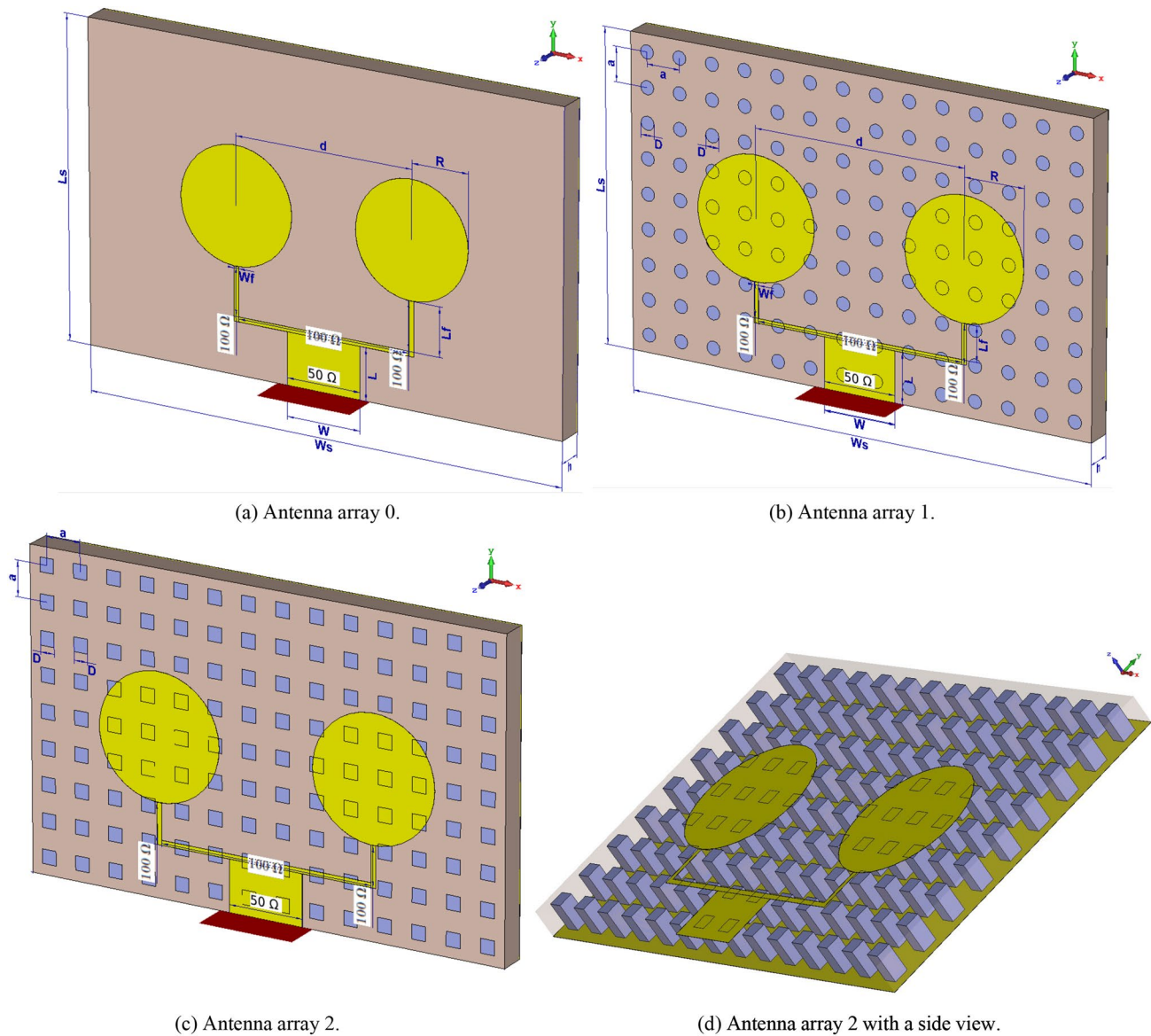


**Fig. 2** The geometry of the proposed antenna arrays based on the homogeneous and periodic PBG substrates

than 286 GHz. Finally, antenna array 2 resonated exactly at the frequency of 0.65 THz with a minimal return loss of  $-74.10$  dB and achieved the largest bandwidth which is greater than 290 GHz. Thus, there was a noticeable improvement in the return loss and the bandwidth after employing the photonic crystal substrate. The gain and radiation efficiency versus the frequency of all the designed antenna arrays in the frequency range of 0.58–0.70 THz are shown in Fig. 4a and Fig. 4b, respectively. The results clearly showed that the gain and radiation efficiency were enhanced for antenna array 1 and antenna array 2 based on periodic photonic crystals substrate. So, antenna array 2 achieved the maximum gain and radiation efficiency in this section with the values of 10.57 dB (20.11%) and 82.96%, respectively at

0.65 THz, then, antenna array 1 achieved a gain of 10.35 dB (17.61%) and radiation efficiency of 81.96% at 0.637 THz, compared to antenna array 0 based on a homogeneous substrate that obtained a gain of 8.80 dB and radiation efficiency of 80.55 % at 0.63 THz.

Figure 5 shows the radiation pattern in dB for the proposed antenna arrays at their resonant frequencies in the plane containing the solid angle  $\theta$  at which the maximum radiation was achieved. The maximum radiation in the pattern of antenna array 0 occurred at  $\theta = 45^\circ$  with a directivity of 9.74 dBi. Then, the maximum radiation in the pattern of antenna array 1 occurred at  $\theta = 39^\circ$  with a directivity of 11.20 dBi. Finally, the maximum radiation in the pattern of antenna array 2 occurred at  $\theta = 40^\circ$  with maximum

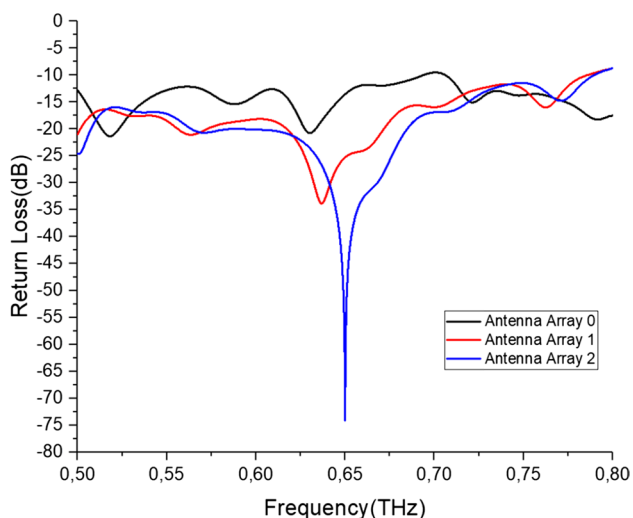


**Fig. 3** Return loss versus the frequency of the proposed antenna arrays

directivity in this section of 11.40 dBi. The directivity has increased a lot after employing the photonic crystal substrate also it is noticed that the side lobes were increased at some angles with higher directivity compared to the homogeneous substrate. Therefore, considering the obtained results, the performance of the proposed antenna array improved by using photonic crystals. Also, it could be worth interesting to observe that by using air cuboids holes embedded in the substrate, an extra performance is observed compared to the air cylinders holes embedded in the substrate as found in antenna array 2 and antenna array 1, respectively, due to the reflection of electromagnetic waves falling in the non-transmission range.

For more clarity, the radiation characteristics of a single element patch such as return loss, bandwidth, gain, and radiation efficiency are shown in Fig. 6. Antenna 1 is the single element patch of antenna array 1, which is designed based on periodic air cylinders holes. Antenna 2 is the single element patch of antenna array 2, which is designed based on periodic air cuboids holes. So, antenna 1 offers at a resonant frequency of 0.65 THz a return loss of  $-27.73$  dB, a bandwidth greater than 213 GHz, a gain of 7.75 dB, and radiation efficiency of 78.96 %, whereas, antenna 2 offers at a resonant frequency of 0.656 THz a return loss of  $-31.42$  dB, a bandwidth greater than 209 GHz, a gain of 7.92 dB, and radiation efficiency of 79.32 %. Clearly that the performance of an array antenna outperforms a single element patch in terms of return loss, bandwidth, gain, and radiation efficiency.

### 3 Antenna array performance investigation

In this section, and in order to enhance the gain, two other antenna arrays were designed based on the structures of antenna array 1 and antenna array 2, but the substrate included mixed air cylinders holes and air cuboids holes at the same time which is divided into several sets, where each set of air cylinders holes and air cuboids holes had different diameters, as shown in Fig. 7. Therefore, Fig. 7a shows antenna array 3 with five sets of air cuboids holes and four sets of air cylinders holes that are horizontally different, where the values of diameters are  $D1=52 \mu\text{m}$ ,  $D2=36 \mu\text{m}$ ,  $D3=60 \mu\text{m}$ ,  $D4=48.26 \mu\text{m}$ ,  $D5=48 \mu\text{m}$ ,  $D6=10 \mu\text{m}$ ,  $D7=30 \mu\text{m}$ ,  $D8=70 \mu\text{m}$ , and  $D9=34 \mu\text{m}$ . Fig. 7b shows antenna array 4 with seven sets of air

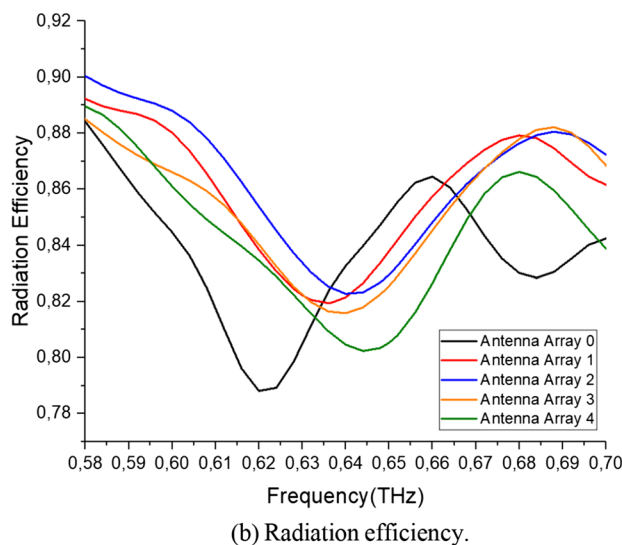
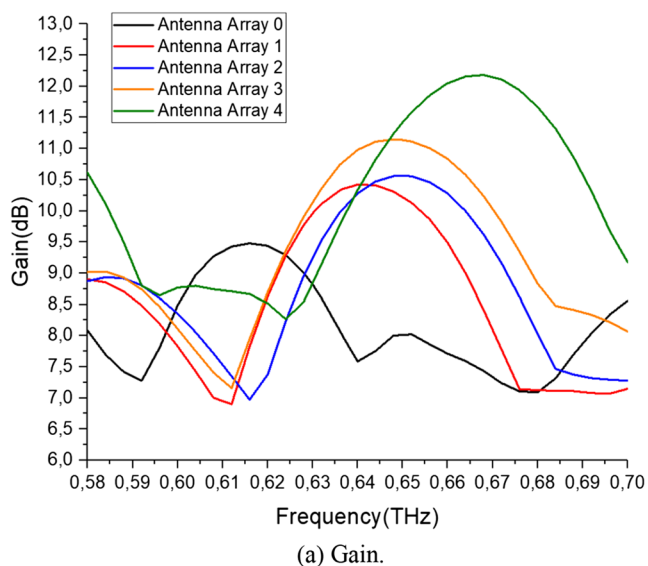


**Fig. 4** Gain and radiation efficiency of all proposed antenna arrays in the frequency range of 0.58–0.70 THz

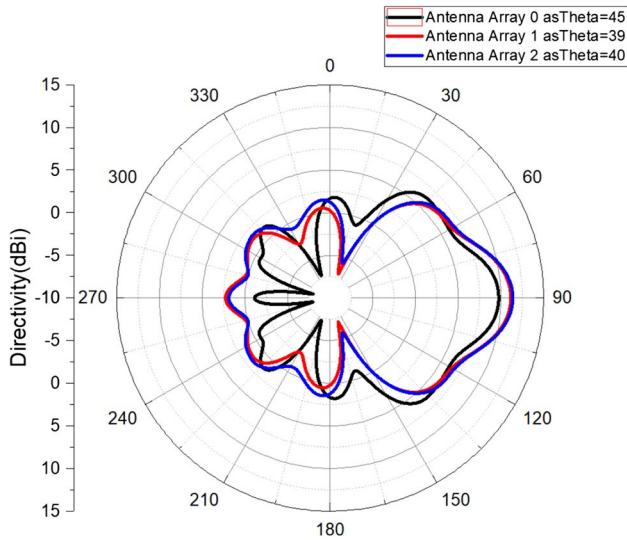


**Fig. 5** The radiation pattern of proposed antenna arrays based on the periodic photonic crystals and the homogeneous substrate at their resonant frequencies for the  $\theta$  plane, which defines the solid angle of the maximum radiation

cylinders holes and air cuboids holes that are vertically different, where the values of diameters are  $D1=98 \mu\text{m}$ ,  $D2=14 \mu\text{m}$ ,  $D3=90 \mu\text{m}$ ,  $D4=11.38 \mu\text{m}$ ,  $D5=86 \mu\text{m}$ ,  $D6=38 \mu\text{m}$ ,  $D7=50 \mu\text{m}$ ,  $D8=42 \mu\text{m}$ ,  $D9=40 \mu\text{m}$ ,  $D10=100 \mu\text{m}$ ,  $D11=18 \mu\text{m}$ ,  $D12=70 \mu\text{m}$ ,  $D13=10 \mu\text{m}$ , and  $D14=100 \mu\text{m}$ . We compare the performance of antenna arrays 3 and 4 to the performance of antenna arrays 1 and 2 in order to see the effect of the non-periodic photonic crystal substrate on the gain and antenna array performance in the THz frequency band.

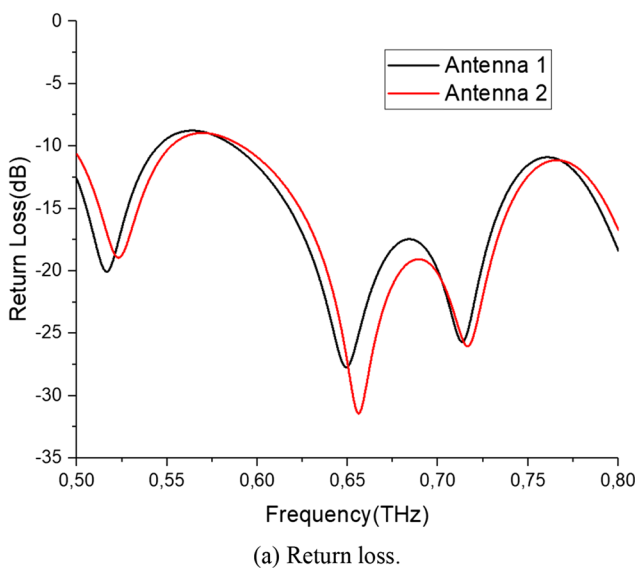
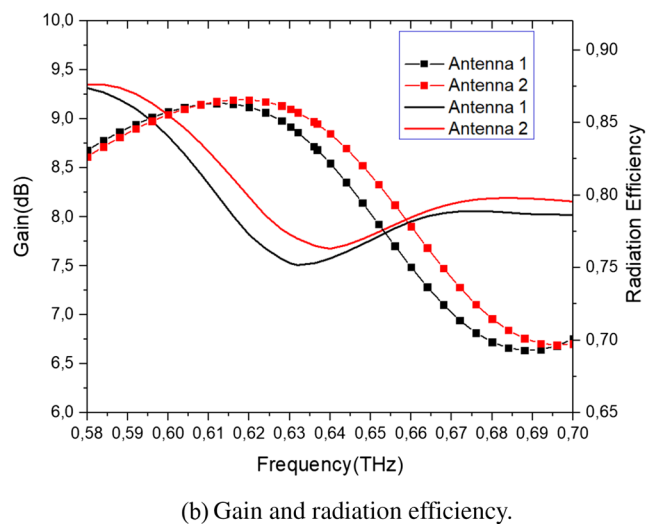


Figure 8 shows the return loss of the proposed antenna arrays based on the photonic crystals versus the frequency, the resonant frequency is that frequency where most of the power fed goes to the radiated patch when the best impedance matching happens between the feed line and the radiated patch with very less power being reflected back. Antenna arrays 3 and 4 have almost the same resonance frequency due to the symmetrical structures with the same feeding method. Therefore, antenna array 3 resonated at the desired frequency of 0.65 THz with a minimal return loss of  $-69.04 \text{ dB}$ , bandwidth greater than 287 GHz, and radiation efficiency 82.56%. Whereas, antenna array 4 resonated at 0.66 THz with a minimal return loss of  $-70.14 \text{ dB}$ , bandwidth greater than 282 GHz, and radiation efficiency 82.52%.

Figure 9 depicts the VSWR performance of the proposed antenna arrays. At their resonant frequencies, antenna array 0 obtained VSWR of 1.2. Whereas, antenna arrays 1, 2, 3, and 4 obtained the values of 1.042, 1.0004, 1.0007, and 1.0006, respectively. The achieved values of VSWR are less than 2, which satisfied the condition for perfect impedance matching. The ideal value of VSWR should be equal to 1 which means 100 % power is accepted and zero reflection [49].

Figure 10 shows the input impedance characteristic of the proposed antenna arrays, which defines impedance matching between the input signal and the feed line. At their resonant frequencies, the input impedance of antenna arrays 0, 1, 2, 3, and 4 are  $54.86 \Omega$  in the real part and  $9 \Omega$  in the imaginary part,  $59.28 \Omega$  in the real part and  $2.18 \Omega$  in the imaginary part,  $60.34 \Omega$  in the real part and  $-0.02 \Omega$  in the imaginary part,  $60.27 \Omega$  in the real part and  $-0.023 \Omega$  in the imaginary



**Fig. 6** Single patch element performance based on photonic crystals

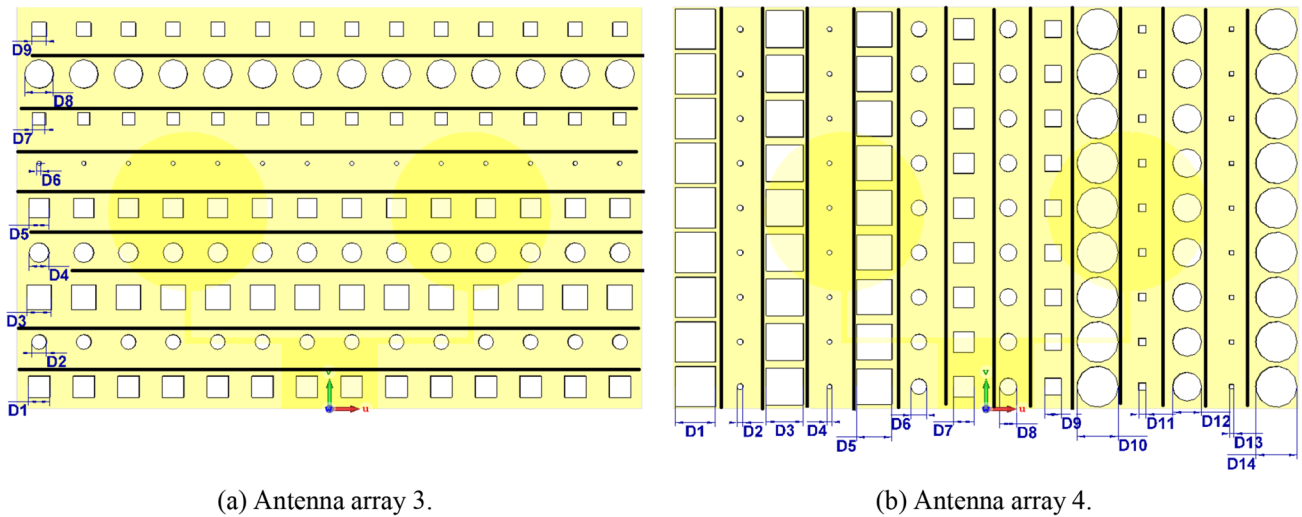


Fig. 7 Geometry of the proposed antenna arrays based on non-periodic photonic crystals

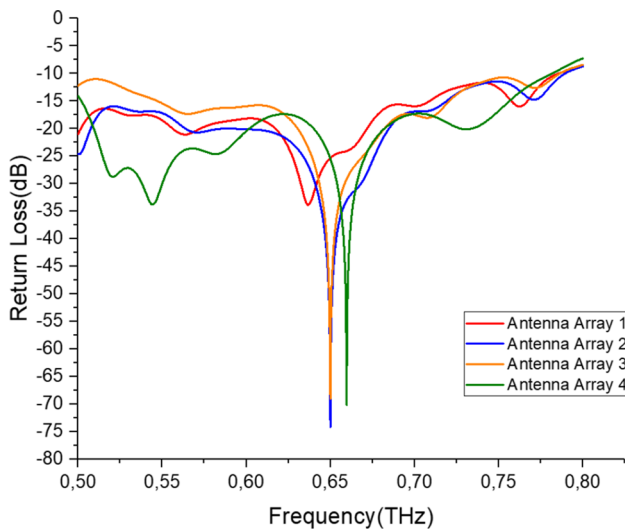


Fig. 8 Return loss of proposed antenna arrays based on photonic crystals versus the frequency

part and  $60.43 \Omega$  in the real part and  $0.011 \Omega$  in the imaginary part, respectively. The value of the input impedance should be around  $50 \Omega$  in real and around  $0 \Omega$  in imaginary to properly match the input signal and the feed line [50].

There was a remarkable enhancement in the gain by using non-periodic photonic crystals substrate compared to periodic photonic crystals substrate and the homogeneous substrate. Thus, antenna array 3 achieved a gain of 11.14 dB with enhancements of 5.4, 7.63, and 26.60%, compared to antenna arrays 2, 1, and 0, respectively. Finally, antenna array 4 achieved the highest gain among all designed antenna arrays of 12.03 dB with enhancements of 13.81, 16.23, and 36.70% compared to antenna arrays 2, 1, and 0, respectively. The reason why antenna array 4 achieves the highest gain

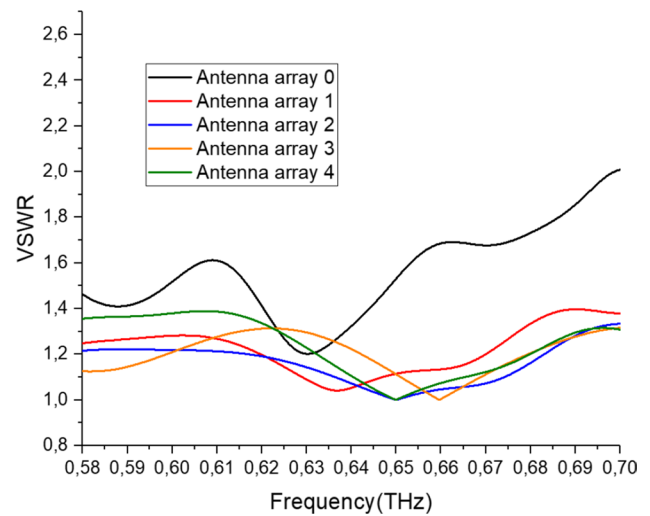
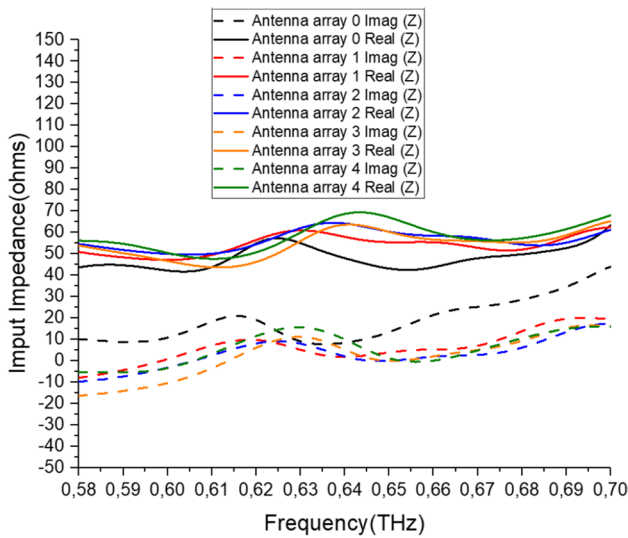


Fig. 9 VSWR of the proposed antenna arrays

in this work, is because antenna array 4 has more sets of optimized air holes compared to antenna arrays 1, 2, and 3. Also, more sets of optimized air holes with different diameters create a discontinuity in the substrate which reduces the dielectric permittivity, thereby causing dielectric loss and conductor loss. These losses will definitely contribute to a drop in radiation efficiency. The radiation characteristics such as return loss, bandwidth, and radiation efficiency of antenna arrays 3 and 4 remained close to the maximum radiation characteristics that were achieved by antenna array 2, however, the gain was enhanced after employing non-periodic photonic crystals substrate.

Figure 11 shows the effect on the gain with similar and different diameters for mixed air cylinders and air cuboids in antenna arrays 3 and 4, the value of the diameters has



**Fig. 10** The input impedance characteristics of the proposed antenna arrays

been varied from 5 to 45  $\mu\text{m}$ , clearly that the gain of antenna arrays 3 and 4 strongly depends on the diameters of the air cylinders and the air cuboids, furthermore, distinct diameters leads to higher gain.

Since the gain and directivity are proportionally related, an enhancement in the directivity also is noticed. Therefore, the maximum directivity is achieved by antenna array 4 of 12.90 dBi where the maximum radiation in the pattern occurred at  $\theta = 40^\circ$ , whereas, antenna array 3 achieved a directivity of 12 dBi where the maximum radiation in the

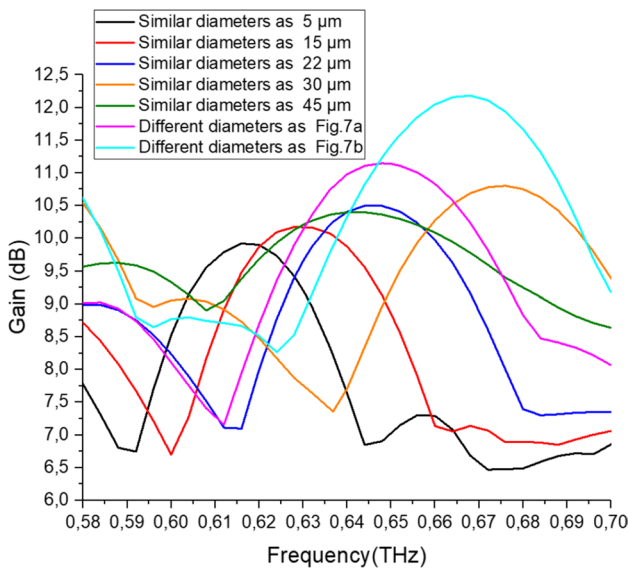


**Fig. 11** Effect of diameters of the photonic crystals on the gain of antenna arrays 3 and 4

pattern occurred at  $\theta = 39^\circ$ . The far-field radiation patterns are shown in Fig. 12 for all designed antenna arrays based on the photonic crystal substrate.

Figure 13 displayed the surface current distribution of the proposed antenna arrays 0, 1, 2, 3, and 4 at their resonant frequencies with the phase of 120. It can be seen that the surface current distribution is sort of arrows, which is intense in the transmission line and radiated patches edges towards the direction of the y-plane. The surface current distribution is also presented in the substrate due to the fact that the simulated polyimide substrate is a lossy dielectric. The utilization of the periodic and non-periodic photonic crystal structures reduces the effective permittivity of the substrate which leads to a different variation of the surface current distribution.

The simulation results indicated that the performance of the proposed antenna array based on the photonic crystal substrate containing air cylinders holes and air cuboids holes improved in terms of the return loss, bandwidth, gain, and radiation efficiency due to the suppression of the surface waves that are found in the conventional antenna array based on a homogeneous substrate. The novelty of this study is the enhancement of the antenna array gain by using mixed air cylinders holes and air cuboids holes embedded in the substrate as shown in Fig. 7 causing more suppression of the undesirable excited surface waves in the substrate which enhances the gain. These results showed that the shape of the photonic crystal has an influence on the antenna array performance. The proposed antenna arrays based on periodic and non-periodic photonic crystal substrates exhibit larger bandwidth and

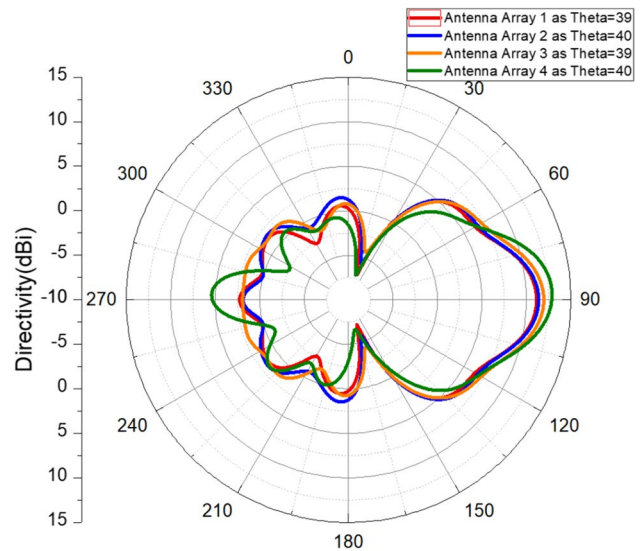


**Fig. 12** The radiation pattern of the proposed antenna arrays based on periodic and non-periodic photonic crystals at their resonant frequencies



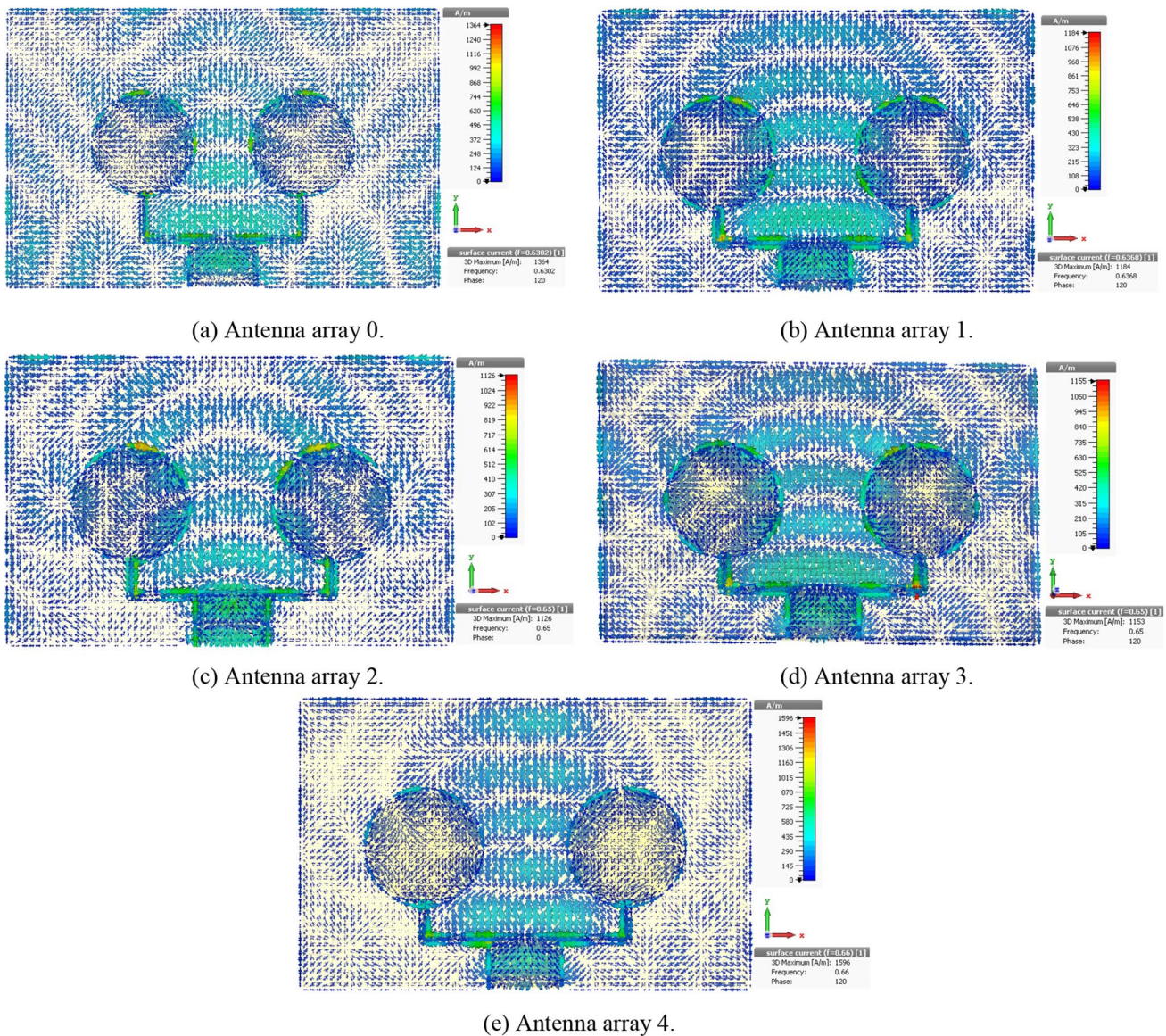


**Fig. 13** Surface current distribution of the proposed antenna arrays at their resonant frequencies with the phase of 120

higher gain with resonance frequencies close to the desired frequency of 0.65 THz as required for the next-generation wireless communication technologies and other interesting applications.

Table. 2 presented the overall radiation characteristics of the proposed antenna arrays in comparison with previously reported works. The highest gain achieved in this study was 12.03 dB which shows superior performance compared with the results of existing antennas in the literature with the enhancements of 51.51% [28], 34.41% [34], 30.90% [34], 208.46% [46], 27.30% [47], 77.10% [48], and most interestingly 36.70% compared to the antenna array 0 based on the homogeneous substrate.

### 4 Conclusion

In this study, photonic crystal and homogeneous substrate structure with a novel  $1 \times 2$  circular microstrip patch antenna array have been studied and compared around 0.65 THz in terms of return loss, bandwidth, gain, and radiation efficiency. The effects of the photonic crystal have been investigated by using air cylinders holes and air cuboids holes embedded in a thick polyimide substrate. The simulation results showed that the best radiation characteristics were achieved when the air cuboids holes are employed as found in antenna array 2 which achieved a minimal return loss of  $-74.10$  dB,

**Table 2** Comparison of the proposed designed antenna arrays and previously reported designs

	$f_r$ (THz)	$S_{11}$ (dB)	BW (GHz)	Gain(dB)	Directivity(dBi)	Rad. eff (%)
[28]	0.6308	−56.81	36.23	7.945	8.612	85.71
[34]	0.63	−56.81	≫ 230	8.95	–	89.31
[34]	0.61	−83.73	≫ 230	9.19	–	90.84
[46]	0.472	−39	435	3.9	–	84
[47]	0.63	−59.15	29.79	9.45	9.99	90.6
[48]	0.69	−64.16	26.7	6.793	6.914	85.78
Antenna array 0	0.63	−20.75	≫ 194	8.80	9.74	80.55
Antenna array 1	0.637	−33.85	≫ 286	10.35 (17.61%)	11.20	81.96
Antenna array 2	0.65	−74.10	≫ 290	10.57 (20.11%)	11.40	82.96
Antenna array 3	0.65	−69.04	≫ 287	11.14 (26.60%)	12	82.56
Antenna array 4	0.66	−70.14	≫ 282	12.03 (36.70%)	12.90	82.54

bandwidth larger than 290 GHz, a gain of 10.57 dB, and radiation efficiency of 82.96%. Next, a novel technique for the gain enhancement of the proposed antenna array is done by mixing the air cylinders holes with the air cuboids holes with a modified diameter value. This technique resulted in an enhancement in the gain as found in antenna array 4 which achieved a gain of 12.03 dB. Hence, the proposed antenna arrays are suitably employed for imaging, sensing, and next-generation wireless communication technologies.

**Acknowledgements** This study was supported by the Algerian Ministry of Higher Education and Scientific Research through funding for PRFU Project

**Data availability** My manuscript has no associated data.

## References

- Skvortsov, L. (2014). Standoff detection of hidden explosives and cold and fire arms by terahertz time-domain spectroscopy and active spectral imaging. *Journal of Applied Spectroscopy*, 81(5), 725–749.
- Naftaly, M., Foulds, A., Miles, R., & Davies, A. (2005). Terahertz transmission spectroscopy of nonpolar materials and relationship with composition and properties. *International Journal of Infrared and Millimeter Waves*, 26(1), 55–64.
- Biabanifard, M., & Abrishamian, M. S. (2018). Circuit modeling of tunable terahertz graphene absorber. *Optik*, 158, 842–849.
- Cherry, S. (2004). Edholm's law of bandwidth. *IEEE spectrum*, 41(7), 58–60.
- Ahmad, N., Mahmoud, S. T., Purohit, G., & Khan, F. (2018). Two color laser self focusing and terahertz generation in multi-ion species plasma. *Optik*, 158, 1533–1542.
- Fitch, M. J., & Osiander, R. (2004). Terahertz waves for communications and sensing. *Johns Hopkins APL technical digest*, 25(4), 348–355.
- Tonouchi, M. (2007). Cutting-edge terahertz technology. *Nature photonics*, 1(2), 97–105.
- N. Salmon, A. Luukanen, R. Appleby, and M. Kemp (2012) Millimeter-wave and terahertz imaging in security applications.
- Taylor, Z. D., Singh, R. S., Bennett, D. B., Tewari, P., Kealey, C. P., Bajwa, N., Culjat, M. O., Stojadinovic, A., Lee, H., Hubschman, J.-P., et al. (2011). Thz medical imaging: In vivo hydration sensing. *IEEE transactions on terahertz science and technology*, 1(1), 201–219.
- Reid, C. B., Pickwell-MacPherson, E., Laufer, J. G., Gibson, A. P., Hebden, J. C., & Wallace, V. P. (2010). Accuracy and resolution of thz reflection spectroscopy for medical imaging. *Physics in Medicine and Biology*, 55(16), 4825.
- Emtsev, K. V., Bostwick, A., Horn, K., Jobst, J., Kellogg, G. L., Ley, L., & Seyller, T. (2009). Towards wafer-size graphene layers by atmospheric pressure graphitization of silicon carbide. *Nature materials*, 8(3), 203–207.
- Woolard, D. L., Jensen, J. O., & Hwu, R. J. (2007). *Terahertz science and technology for military and security applications*. World Scientific.
- Liu, H.-B., Zhong, H., Karpowicz, N., Chen, Y., & Zhang, X.-C. (2007). Terahertz spectroscopy and imaging for defense and security applications. *Proceedings of the IEEE*, 95(8), 1514–1527.
- K Fan Z-C Hao W Hong (2016) A 325–500 ghz high gain antenna for terahertz applications, In 2016 *International Symposium on Antennas and Propagation (ISAP)* IEEE pp. 780–781
- Zarrabi, F. B., Seyedsharbaty, M. M., Ahmed, Z., Arezoomand, A. S., & Heydari, S. (2017). Wide band yagi antenna for terahertz application with graphene control. *Optik*, 140, 866–872.
- Runge, M., Engel, D., Schneider, M., Reimann, K., Woerner, M., & Elsaesser, T. (2020). Spatial distribution of electric field enhancement across the gap of terahertz bow-tie antennas. *Optics Express*, 28(17), 389–398.
- Formanek, F., Brun, M.-A., Umetsu, T., Omori, S., & Yasuda, A. (2009). Aspheric silicon lenses for terahertz photoconductive antennas. *Applied Physics Letters*, 94(2), 021113.
- Cahill, R. (1989). Design of core support mechanism for mm-wave di-electrically loaded horn. *Electronics Letters*, 25(18), 1248–1249.
- Khamaisi, B., Jameson, S., & Socher, E. (2013). A 210–227 ghz trans-mitter with integrated on-chip antenna in 90 nm cmos technology. *IEEE Transactions on Terahertz Science and Technology*, 3(2), 141–150.
- Malhotra, I., Jha, K. R., & Singh, G. (2017). Analysis of highly directive photoconductive dipole antenna at terahertz frequency for sensing and imaging applications. *Optics Communications*, 397, 129–139.
- Han, K., Nguyen, T. K., Park, I., & Han, H. (2010). Terahertz yagi-uda antenna for high input resistance. *Journal of Infrared, Millimeter, and Terahertz Waves*, 31(4), 441–454.
- Mangeney, J. (2012). Thz photoconductive antennas made from ion-bombarded semiconductors. *Journal of Infrared, Millimeter, and Terahertz Waves*, 33(4), 455–473.
- Howell, J. (1975). Microstrip antennas. *IEEE Transactions on Antennas and Propagation*, 23(1), 90–93.

24. Mailloux, R., McIlvenna, J., & Kernweis, N. (1981). Microstrip array technology. *IEEE Transactions on Antennas and Propagation*, 29(1), 25–37.
25. Liu, N.-W., Zhu, L., Choi, W.-W., & Zhang, J.-D. (2018). A low-profile differentially fed microstrip patch antenna with broad impedance bandwidth under triple-mode resonance. *IEEE Antennas and Wireless Propagation Letters*, 17(8), 1478–1482.
26. Tse, D., & Viswanath, P. (2005). *Fundamentals of wireless communication*. Cambridge University Press.
27. Kazemi, F. (2020). Dual band compact fractal thz antenna based on crlhl and graphene loads. *Optik*, 206, 164369.
28. Kushwaha, R. K., Karuppanan, P., & Malviya, L. (2018). Design and analysis of novel microstrip patch antenna on photonic crystal in thz. *Physica B: Condensed Matter*, 545, 107–112.
29. M. V. Hidayat and C. Apriono (2019) Simulation of terahertz imaging using microstrip linear array antenna for breast cancer detection, In *AIP conference proceedings*, 2092(1), pp. 020020, AIP Publishing LLC
30. Azarbar, A., Masouleh, M., & Behbahani, A. (2014). A new terahertz microstrip rectangular patch array antenna. *International Journal of Electromagnetics and Applications*, 4(1), 25–29.
31. Shukla, S., & Ojha, S. S. Review of various techniques available to modify parameters of microstrip patch antenna.
32. Sirmaci, Y. D., Akin, C. K., & Sabah, C. (2016). Fishnet based metamaterial loaded thz patch antenna. *Optical and Quantum Electronics*, 48(2), 168.
33. Cheng, C., Lu, Y., Zhang, D., Ruan, F., & Li, G. (2020). Gain enhancement of terahertz patch antennas by coating epsilon-near-zero metamaterials. *Superlattices and Microstructures*, 139, 106390.
34. Hocini, A., Temmar, M. N., Khedrouche, D., & Zamani, M. (2019) Novel approach for the design and analysis of a terahertz microstrip patch antenna based on photonic crystals, *Photonics and Nanostructures-Fundamentals and Applications*, 36, 100723.
35. Temmar, M. N. E., Hocini, A., Khedrouche, D., & Zamani, M. (2019). Analysis and design of a terahertz microstrip antenna based on a synthesized photonic bandgap substrate using bps. *Journal of Computational Electronics*, 18(1), 231–240.
36. eddineTemmar, M. N., Hocini, A., Khedrouche, D., & Denidni, T. A. (2020). Enhanced flexible terahertz microstrip antenna based on modified silicon-air photonic crystal". *Optik*, 217, 164897.
37. Temmar, M. N. E., Hocini, A., Khedrouche, D., & Denidni, T. A. (2021) Analysis and design of mimo indoor communication system using terahertz patch antenna based on photonic crystal with graphene. *Photonics and Nanostructures-Fundamentals and Applications*, 43, 100867.
38. Sharma, A., Dwivedi, V. K., & Singh, G. (2008). *Thz rectangular patch microstrip antenna design using photonic crystal as substrate*, In *Progress in Electromagnetic Research Symposium* (pp. 161–165). Cambridge.
39. Semouchkina, E., Duan, R., Gandji, N. P., Jamilan, S., Semouchkin, G., & Pandey, R. (2016). Superluminal media formed by photonic crystals for transformation optics-based invisibility cloaks. *Journal of Optics*, 18(4), 044007.
40. A. I. Il'in, V. T. Volkov, O. V. Trofimov, and M. Y. Barabanenkov (2015) Technological problems in forming si waveguide lamellar diffraction gratings and 2d photonic crystals by plasma and wet etching of si, In *2015 IEEE 15th International Conference on Nanotechnology (IEEE-NANO)*. IEEE, pp. 983–986.
41. Singh, K. K., & Gupta, S. C. (2013). Design and Simulation of Microstrip patch array antenna for C Band Application at IMT (4400-4900 MHz) advanced spectrum with Series feed and parallel feed. *International Journal of Scientific & Engineering Research*, 4(12).
42. Benlakehal, M. E., Hocini, A., Khedrouche, D., Temmar, M. N. E., & Denidni, T. A. (2022). Design and analysis of a 2 x 2 microstrip ratch antenna array based on periodic and non-periodic photonic crystals substrate in THz. *Optical and Quantum Electronics*, 54(3).
43. Sharma, S., Tripathi, C., & Rishi, R. (2017). Impedance matching techniques for microstrip patch antenna. *Indian Journal of Science and Technology*, 10(28), 1–16.
44. Benlakehal, M. E., Hocini, A., Khedrouche, D., Denidni, T. A., et al. (2022). Design and analysis of novel microstrip patch antenna array based on photonic crystal in thz. *Optical and Quantum Electronics*, 54(5), 1–16.
45. Rabbani, M. S., & Ghafouri-Shiraz, H. (2017). Liquid crystalline polymer substrate-based thz microstrip antenna arrays for medical applications. *IEEE Antennas and Wireless Propagation Letters*, 16, 1533–1536.
46. Vasu Babu, K., Das, S., Varshney, G., Sree, G. N. J., & Madhav, B. T. P. (2022). A micro-scaled graphene-based tree-shaped wide-band printed mimo antenna for terahertz applications. *Journal of Computational Electronics*, 21(1), 289–303.
47. Ahmad, I., Ullah, S., Ullah, S., Habib, U., Ahmad, S., Ghaffar, A., & Limiti, E. (2021). Design and analysis of a photonic crystal based planar antenna for thz applications. *Electronics*, 10(16), 1941.
48. Ullah, S., Ruan, C., Haq, T. U., & Zhang, X. (2019). High performance thz patch antenna using photonic band gap and defected ground structure. *Journal of Electromagnetic Waves and Applications*, 33(15), 1943–1954.
49. Singh, A., & Singh, S. (2015). A trapezoidal microstrip patch antenna on photonic crystal substrate for high speed THz applications. *Photonics and Nanostructures-Fundamentals and applications*, 14, 52–62.
50. Shamim, S., Uddin, M. S., Hasan, M., Samad, M., et al. (2021). Design and implementation of miniaturized wideband microstrip patch antenna for high-speed terahertz applications. *Journal of Computational Electronics*, 20(1), 604–610.

**Publisher's Note** Springer Nature remains neutral with regard to jurisdictional claims in published maps and institutional affiliations.

Springer Nature or its licensor (e.g. a society or other partner) holds exclusive rights to this article under a publishing agreement with the author(s) or other rightsholder(s); author self-archiving of the accepted manuscript version of this article is solely governed by the terms of such publishing agreement and applicable law.



**Mohamed Elamine Benlakehal** was born in Medea, Algeria, in 1995. He received the Bachelor degree in electrical and electronics engineering and the Master degree in telecommunications from the Institute of Electrical and Electronic Engineering of Boumerdes, Algeria, in 2017 and 2019, respectively. Currently, he is preparing the doctorate degree in the Faculty of Technology from the University of Boumerdes, Algeria, since October 2019. Also, he is a temporary teacher in the Institute of Electrical and Electronic Engineering of Boumerdes.

He published six manuscripts in the journal of Springer in 2022. His research interests include antennas, propagation, terahertz, plasmonic devices, photonic crystals, wireless and mobile communication systems, data processing and artificial intelligence.



**Abdesselam Hocini** Received the Ph.D. in electronics instrumentation in 2008 from Constantine University, Algeria. He is currently a Professor in Department of Electronics at University of Mohamed Boudiaf of M'sila, Algeria. His research interests include the design and characterization of photonic devices. In particular, his research concerns sensing, solar cells and realizing advanced functional photonic crystal devices.



**Djamel Khedrouche** received the Ph.D. in electronics telecommunication from Constantine University, Algeria, in 2009. He is currently a Professor in Department of Electronics at University of Mohamed Boudiaf of M'sila, Algeria. His research interests include the modeling and characterization in electromagnetic and microwave devices. Recently, his research concerns microstrip antennas, UWB antennas and realizing advanced functional metamaterial devices.



**Mohamed Nasr eddine Temmar** was born in Medea, Algeria, in 1994. He received the Bachelor degree in electrical and electronics engineering and the Master degree in telecommunications from the Institute of Electrical and Electronic Engineering of Boumerdes, Algeria, in 2015 and 2017, respectively. He received the doctorate degree from the University of Msila, Algeria, in January 2021. Currently, he is an Adjunct Professor in the University of Medea. His research interests include anten-

nas, propagation, terahertz, plasmonic devices, photonic crystals, wireless and mobile communication systems, data processing and artificial

intelligence. Dr. Temmar is a reviewer of several international journals.



**Tayeb Ahmed Denidni** Received the M.S. and Ph.D. degrees in electrical engineering from Laval University, Quebec, QC, Canada, in 1990 and 1994, respectively. He was a Professor with the Engineering Department, Université du Quebec at Rimouski, Rimouski, QC, Canada, from 1994 to 2000, where he founded the Telecommunications Laboratory. Since 2000, he has been with the Institut National de la Recherche Scientifique (INRS), Université du Quebec, Montreal, QC, Canada.

He found the RF Laboratory, INRSEM, Montreal. He has extensive experience in antenna design and is leading a large research group consisting of three research scientists, eight Ph.D. students, and two M.S. students. His current research interests include reconfigurable antennas using EBG and FSS structures, dielectric resonator antennas, metamaterial antennas, adaptive arrays, switched multi-beam antenna arrays, ultrawideband antennas, microwave, and development for wireless communications systems. He served as an Associate Editor for the IEEE Transactions on Antennas and Propagation, from 2008 to 2010; and the IEEE Antennas and Wireless Propagation Letters, from 2005 to 2007. Since 2015, he has been serving as an Associate Editor for Electronics Letters (IET).